The influence of morphology, AGN and environment on the quenching histories of galaxies

Rebecca Jane Smethurst

Pembroke College

University of Oxford

A thesis submitted for the degree of

Doctor of Philosophy

Michaelmas 2016

This thesis is dedicated to
someone
for some special reason

Acknowledgements

Thank ALLL TEH people.

Abstract

GZ shit happens.

Contents

List of Figures

Chapter 1

Introduction

Previous large scale surveys of galaxies have revealed a bimodality in the colour-magnitude diagram (CMD) with two distinct populations; one at relatively low mass, with blue optical colours and another at relatively high mass, with red optical colours (?Baldry et al., 2006; ?; ?; Brammer et al., 2009). These populations were dubbed the 'blue cloud' and 'red sequence' respectively (????). The Galaxy Zoo project (Lintott et al., 2011), which produced morphological classifications for a million galaxies, helped to confirm that this bimodality is not entirely morphology driven (????Bamford et al., 2009; Skibba et al., 2009), detecting larger fractions of spiral galaxies in the red sequence (?) and elliptical galaxies in the blue cloud (?) than had previously been detected.

The sparsely populated colour space between these two populations, the so-called 'green valley', provides clues to the nature and duration of galaxies' transitions from blue to red. This transition must occur on rapid timescales, otherwise there would be an accumulation of galaxies residing in the green valley, rather than an accumulation in the red sequence as is observed (??). Green valley galaxies have therefore long been thought of as the 'crossroads' of galaxy evolution, a transition population between the two main galactic stages of the star forming blue cloud and the 'dead' red sequence (?????????).

The intermediate colours of these green valley galaxies have been interpreted as evidence for recent quenching (suppression) of star formation (?). Star forming galaxies are observed to lie on a well defined mass-SFR relation, however quenching a galaxy causes it to depart from this relation (??).

By studying the galaxies which have just left this mass-SFR relation, I can probe the quenching mechanisms by which this occurs. There have been many previous theories for the initial triggers of these quenching mechanisms, including negative feedback from AGN (Di Matteo et al., 2005; ?; Nandra et al., 2007; ?), mergers

(Darg et al., 2010; ?; ?), supernovae winds (?), cluster interactions (???) and secular evolution (???). By investigating the *amount* of quenching that has occurred in the blue cloud, green valley and red sequence; and by comparing the amount across these three populations, I can apply some constraints to these theories.

The nature of the observed co-evolution of galaxies and their central supermassive black holes (???) and the effects of AGN feedback on galaxies are two of the most important open issues in galaxy evolution. AGN feedback was first suggested as a mechanism for regulating star formation in simulations (?Croton et al., 2006; ?; ?) and indirect evidence has been observed for both positive and negative feedback in various systems (see the comprehensive review from ?).

The strongest observational evidence for AGN feedback in a population is that the largest fraction of AGN are found in the green valley (?Hickox et al., 2009; ?), suggesting some link between AGN activity and the process of quenching which moves a galaxy from the blue cloud to the red sequence. However, concrete statistical evidence for the effect of AGN feedback on the host galaxy population has so far been elusive.

There are many mechanisms which are proposed to cause quenching; including mergers (?), mass quenching (??), morphological quenching (?) and the environment of a galaxy.

The galaxy environment as a cause of quenching was proposed due to the correlation of both morphology (Dressler, 1980) and the quenched galaxy fraction (?) with environmental density.

BUT does this correlation truly imply causation? Evidence from simulations (?) suggests that the environment may not be the dominant quenching mechanisms for galaxies. Perhaps the correlation of increased galaxy quenched fractions with environment is due to a combination of mergers, mass and morphological quenching. In denser environments, galaxies are more likely to encounter another galaxy in a merger scenario and large viral radii give rise to long infall times during which gas reservoirs can be depleted due to star formation.

To study this I need to look at how quenching timescale changes in groups and clusters of galaxies with different properties in order to isolate the cause of the density-morphology and density-SFR correlations.

1.1 Galaxy Zoo

In this investigation I use visual classifications of galaxy morphologies from the Galaxy Zoo 2[1] citizen science project (Willett et al., 2013), which obtains multiple independent classifications for each galaxy image; the full question tree for each image is shown in Figure 1 of Willett et al. 2013.

The Galaxy Zoo 2 (GZ2) project consists of $304,022$ images from the SDSS DR8 (a subset of those classified in Galaxy Zoo 1; GZ1) all classified by *at least* 17 independent users, with the mean number of classifications standing at ~ 42. The GZ2 sample is more robust than the GZ1 sample and provides more detailed morphological classifications, including features such as bars, the number of spiral arms and the ellipticity of smooth galaxies. It is for these reasons I use the GZ2 sample, as opposed to the GZ1, allowing for further investigation of specific galaxy classes in the future (see Section **??**). The only selection that was made on the sample was to remove objects considered to be stars, artefacts or merging pairs by the users (i.e. with $p_{star/artefact} \geq 0.8$ or $p_{merger} \geq 0.420$; see Willett et al. 2013 Table 3 and discussion for details of this fractional limit). Further to this, I required NUV photometry from the GALEX survey, within which $\sim 42\%$ of the GZ2 sample were observed, giving a total sample size of $126,316$ galaxies. The completeness of this subsample of GZ2 matched to GALEX is shown in Figure **??** with the u-band absolute magnitude against redshift for this sample compared with the SDSS data set. Typical Milky Way L_* galaxies with $M_u \sim -20.5$ are still included in the GZ2 subsample out to the highest redshift of $z \sim 0.25$; however dwarf and lower mass galaxies are only detected at the lowest redshifts.

The first task of GZ2 asks users to choose whether a galaxy is mostly smooth, is featured and/or has a disc or is a star/artefact. Unlike other tasks further down in the decision tree, every user who classifies a galaxy image will complete this task (others, such as whether the galaxy has a bar, is dependent on a user having first classified it as a featured galaxy). Therefore I have the most statistically robust classifications at this level.

The classifications from users produces a vote fraction for each galaxy (the debiased fractions calculated by Willett et al. (2013) were used in this investigation); for example if 80 of 100 people thought a galaxy was disc shaped, whereas 20 out of 100 people thought the same galaxy was smooth in shape (i.e. elliptical), that galaxy would have vote fractions $p_s = 0.2$ and $p_d = 0.8$. In this example this galaxy would

[1] `http://zoo2.galaxyzoo.org/`

be included in the *'clean'* disc sample ($p_d \geq 0.8$) according to Willett et al. (2013) and would be considered a late-type galaxy. All previous Galaxy Zoo projects have incorporated extensive analysis of volunteer classifications to measure classification accuracy and bias, and compute user weightings (for a detailed description of debiasing and consistency-based user weightings, see either Section 3 of Lintott et al. 2009 or Section 3 of Willett et al. 2013).

The classifications are highly accurate and provide a continuous scale of morphological features, as shown in Figure **??**, rather than a simple binary classification separating elliptical and disc galaxies. These classifications allow each galaxy to be considered as a probabilistic object with both bulge and disc components.

Chapter 2

STARPY: A Bayesian analysis of a galaxy's SFH

The work in the following chapter has been published in Smethurst et al. (2015).

In order to achieve robust conclusions we conduct a Bayesian analysis (**??**) of our SFH models in comparison to the observed GZ2 sample data. This approach requires consideration of all possible combinations of $\theta \equiv (t_q, \tau)$. Assuming that all galaxies formed at $t = 0$ Gyr with an initial burst of star formation, we can assume that the 'age' of each galaxy in the GZ2 sample is equivalent to an observed time, t_k^{obs} (see Section **??**). We then use this 'age' to calculate the predicted model colours at this cosmic time for a given combination of θ: $d_{c,p}(\theta_k, t_k^{obs})$ for both optical and NUV ($c = opt, NUV$) colours. We can now directly compare our model colours with the observed GZ2 galaxy colours, so that for a single galaxy k with optical $(u-r)$ colour, $d_{opt,k}$ and NUV $(NUV - u)$ colour, $d_{NUV,k}$, the likelihood $P(d_k|\theta_k, t_k^{obs})$ is:

$$P(d_k|\theta_k, t_k^{obs}) = \frac{1}{\sqrt{2\pi\sigma_{opt,k}^2}} \frac{1}{\sqrt{2\pi\sigma_{NUV,k}^2}} \exp\left[-\frac{(d_{opt,k} - d_{opt,p}(\theta_k, t_k^{obs}))^2}{\sigma_{opt,k}^2}\right] \exp\left[-\frac{(d_{NUV,k} - d_{NUV,p}(\theta_k}{\sigma_{NUV,k}^2}\right. \tag{2.1}$$

We have assumed that $P(d_{opt}|\theta_k, t_k^{obs})$ and $P(d_{NUV}|\theta_k, t_k^{obs})$ are independent of each other and that the errors on the observed colours are also independent. To obtain the probability of each combination of θ values given the GZ2 data: $P(\theta_k|d_k, t^{obs})$, i.e. how likely is a single SFH model given the observed colours of a single GZ2 galaxy, we utilise Bayes' theorem:

$$P(\theta_k|d_k, t^{obs}) = \frac{P(d_k|\theta_k, t^{obs})P(\theta_k)}{\int P(d_k|\theta_k, t^{obs})P(\theta_k)d\theta_k}. \tag{2.2}$$

We assume a flat prior on the model parameters so that:

$$P(\theta_k) = \begin{cases} 1 & \text{if } 0 \leq t_q \text{ [Gyr] } \leq 13.8 \text{ and } 0 \leq \tau \text{ [Gyr] } \leq 4 \\ 0 & \text{otherwise.} \end{cases} \tag{2.3}$$

As the denominator of Equation 2.2 is a normalisation factor, comparison between likelihoods for two different SFH models (i.e., two different combinations of $\theta_k = [t_q, \tau]$) is equivalent to a comparison of the numerators. Calculation of $P(\theta_k|d_k, t^{obs})$ for any θ is possible given galaxy data from the GZ2 sample. Markov Chain Monte Carlo (MCMC; **??**Goodman & Weare 2010) provides a robust comparison of the likelihoods between θ values; here we choose *emcee*,[1] a Python implementation of an affine invariant ensemble sampler by **?**.

This method allows for a more efficient exploration of the parameter space by avoiding those areas with low likelihood. A large number of 'walkers' are started at an initial position where the likelihood is calculated; from there they individually 'jump' to a new area of parameter space. If the likelihood in this new area is greater (less) than the original position then the 'walkers' accept (reject) this change in position. Any new position then influences the direction of the 'jumps' of other walkers. This is repeated for the defined number of steps after an initial 'burn-in' phase. *emcee* returns the positions of these 'walkers', which are analogous to the regions of high probability in the model parameter space. The model outlined above has been coded using the *Python* programming language into a package named STARPY which has been made freely available to download[2]. An example output from this Python package for a single galaxy from the GZ2 sample in the red sequence is shown in Figure 2. The contours show the positions of the 'walkers' in the Markov Chain which are analogous to the areas of high probability.

In order to test that STARPY can find the correct quenching model for a given observed colour, 25 synthesised galaxies were created with known SFHs (i.e. known values of θ) from which optical and NUV colours were generated. These were input into STARPY to ensure that the known values of θ were reproduced, within error, for each of the 25 synthesised galaxies. Figure 2.2 shows the results for each of these 25 synthesised galaxies, with the known values of θ shown by the red lines. In some cases this red line does not coincide with the peak of the distribution shown in the histograms for one parameter, however in all cases the intersection of the red lines is within the sample contours.

[1] `dan.iel.fm/emcee/`
[2] `github.com/zooniverse/starpy`

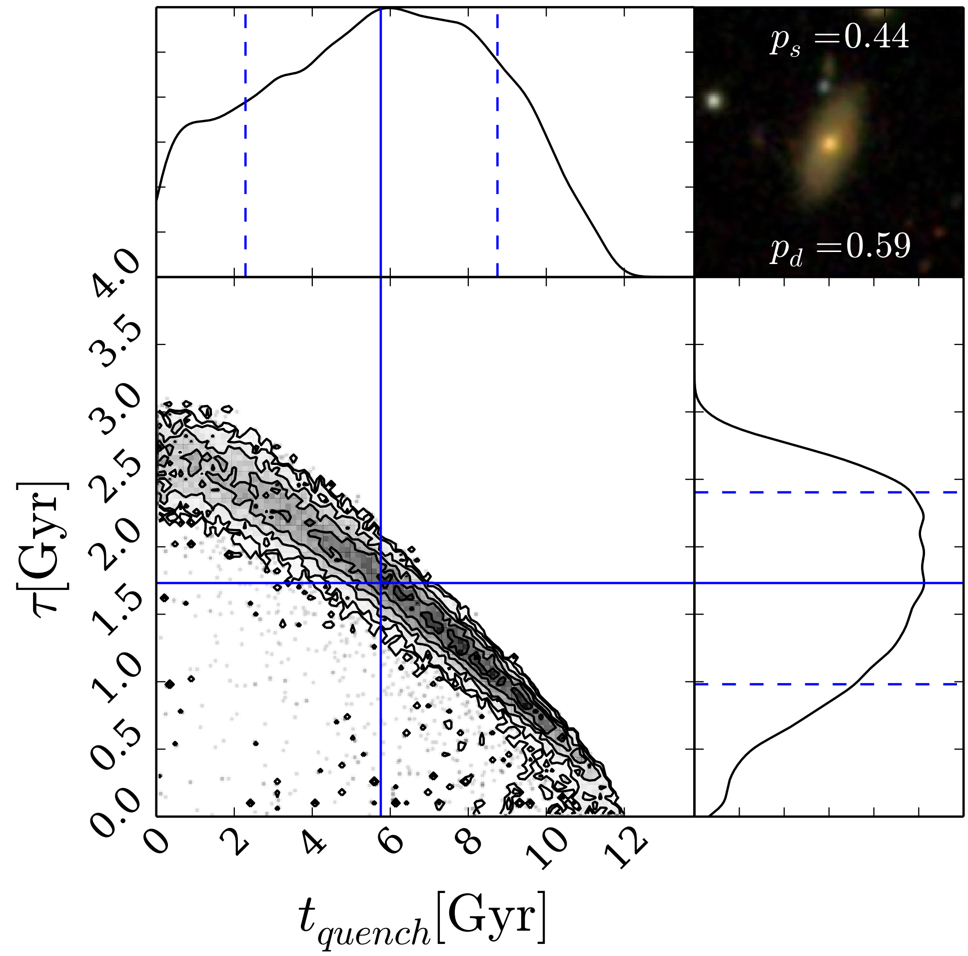

Figure 2.1: Example output from STARPY for a galaxy within the red sequence. The contours show the positions of the 'walkers' in the Markov Chain (which are analogous to the areas of high probability) for the quenching models described by $\theta = [t_q, \tau]$ and the histograms show the 1D projection along each axis. Solid (dashed) blue lines show the best fit model (with $\pm 1\sigma$) to the galaxy data. The postage stamp image from SDSS is shown in the top right along with the debiased vote fractions for smooth (p_s) and disc (p_d) from Galaxy Zoo 2.

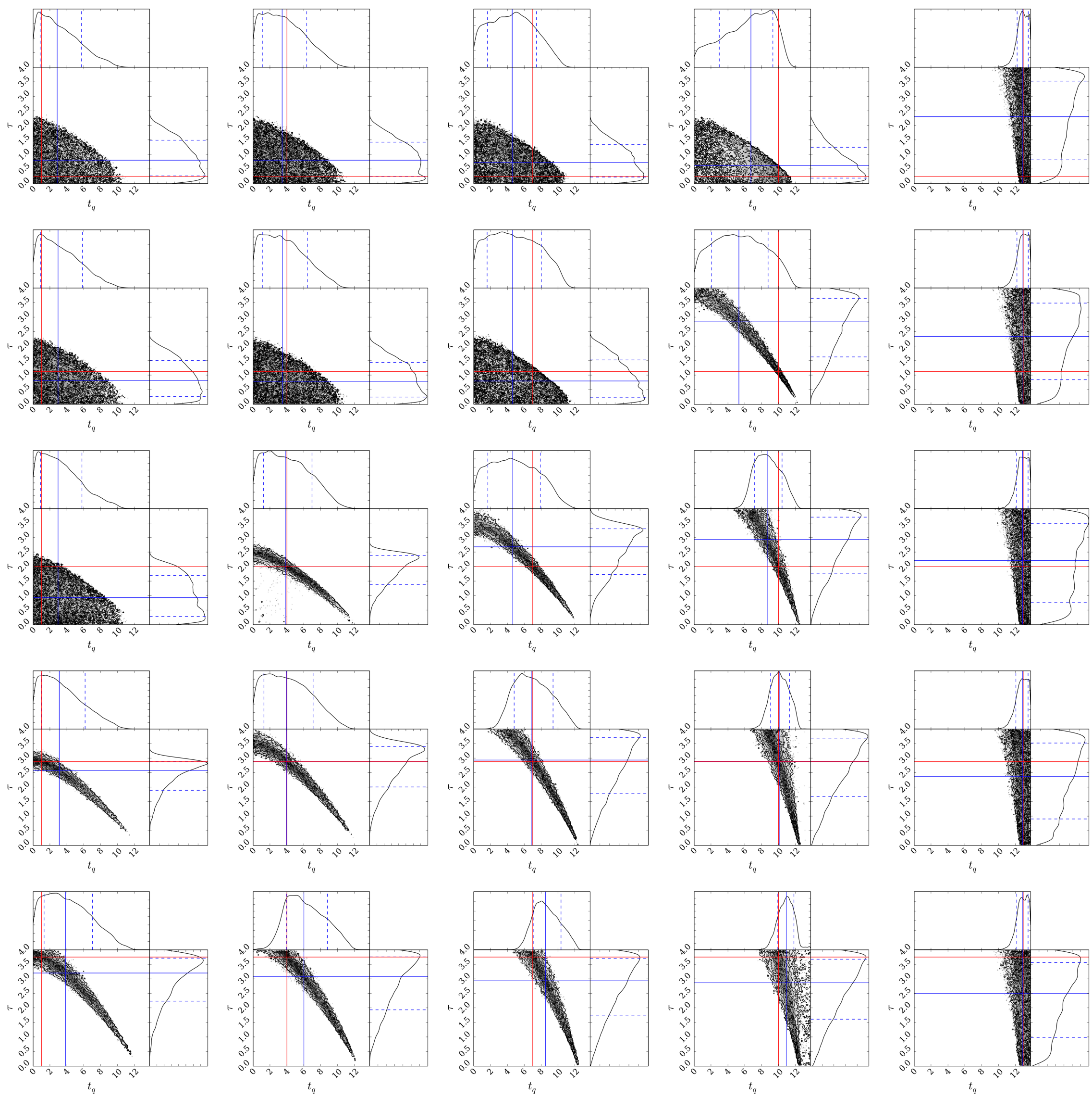

Figure 2.2: Results from STARPY for an array of synthesised galaxies with known, i.e. true, t_q and τ values (marked by the red lines) using the complete function to calculate the predicted colour of a proposed set of θ values in each MCMC iteration, assuming an error on the calculated known colours of $\sigma_{u-r} = 0.124$ and $\sigma_{NUV-u} = 0.215$, the average errors on the GZ sample colours. In each case STARPY succeeds in locating the true parameter values within the degeneracies of the star formation history model. These degeneracies can clearly be seen in Figure **??**.

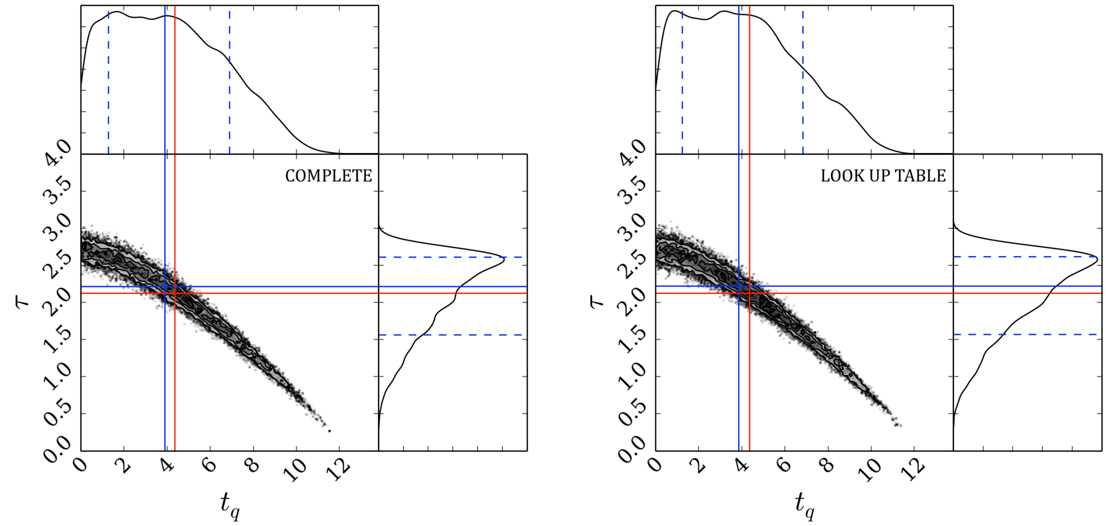

Figure 2.3: Left panel: Results from STARPY for <u>true</u> t_q and τ values (red lines) using the complete function to calculate the predicted colour of a proposed set of θ values in each MCMC iteration. The median walker position (the 50th percentile of the Bayesian probability distribution) is shown by the solid blue line with the dashed lines encompassing $68\%(\pm 1\sigma)$ of the samples (the 16th and 84th percentile positions). The time taken to run for a single galaxy using this method is approximately 2 hours. Right panel: Results from STARPY for <u>true</u> t_q and τ values using a look up table generated from the complete function to calculate the predicted colour of a proposed set of θ values in each MCMC iteration. The time taken to run for a single galaxy using this method is approximately 2 minutes.

We find peaks in the histograms across all areas of the parameter space in both dimensions of $[t, \tau]$, this ensures that the results presented in Figures **??**, **??** & **??** arise due to a superposition of extended probability distributions, as opposed to a bimodal distribution of probability distributions across all galaxies.

Considering the size of the sample in this investigation of $126,316$ galaxies total, a three dimensional look up table (in observed time, quenching time and quenching rate) was generated using the star formation history function in STARPY to speed up the run time.

We wish to consider the model parameters for the populations of galaxies across the colour magnitude diagram for both smooth and disc galaxies, therefore we run the STARPY package on each galaxy in the GZ2 sample. This was extremely time consuming; for each combination of θ values which *emcee* proposes, a new SFH must be built, prior to convolving it with the BC03 SPS models at the observed age and then predicted colours calculated from the resultant SED. For a single galaxy this

Table 2.1: Median walker positions (the 50th percentile; as shown by the blue solid lines in Figure 2.3) found by STARPY for a single galaxy, using the complete star formation history function and a look up table to speed up the run time. The errors quoted define the region in which 68% of the samples are located, shown by the dashed blue lines in Figure 2.3. The known true values are also quoted, as shown by the red lines in Figure 2.3. All values are quoted to three significant figures.

	t_q	τ
True	4.37	2.12
Complete	$3.893\pm^{3.014}_{2.622}$	$2.215\pm^{0.395}_{0.652}$
Look up table	$3.850\pm^{2.988}_{2.619}$	$2.218\pm^{0.399}_{0.649}$

takes up to 2 hours on a typical desktop machine for long Markov Chains. A look-up table was therefore generated at 50 t^{obs}, for 100 t_{quench} and 100 τ values; this was then interpolated over for a given observed galaxy's age and proposed θ values at each step in the Markov Chain. This ensures that a single galaxy takes approximately 2 minutes to run on a typical desktop machine. Figure 2.3 shows an example of how using the look up table in place of the full function does not affect the results to a significant level. Table 2 quotes the median walker positions (the 50th percentile of the Bayesian probability distribution) along with their $\pm1\sigma$ ranges for both methods in comparison to the true values specified to test STARPY. The uncertainties incorporated into the quoted values by using the look up table are therefore minimal with a maximum $\Delta = 0.043$.

Using this lookup table, each of the $126,316$ total galaxies in the GZ2 sample was run through STARPY on multiple cores of a computer cluster to obtain the Markov Chain positions (analogous to $P(\theta_k|d_k)$) for each galaxy, k (see Figure 2). In each case the Markov Chain consisted of 100 'walkers' which took 400 steps in the 'burn-in' phase and 400 steps thereafter, at which point the MCMC acceptance fraction was checked to be within the range $0.25 < f_{acc} < 0.5$ (which was true in all cases). Due to the Bayesian nature of this method, a statistical test on the results is not possible; the output is probabilistic in nature across the entirety of the parameter space.

These individual galaxy positions are then combined to visualise the areas of high probability in the model parameter space across a given population (e.g. the green valley).

We discard walker positions returned by STARPY with a corresponding probability of $P(\theta_k|d_k) < 0.2$ in order to exclude galaxies which are not well fit by the quenching model; for example blue cloud galaxies which are still star forming will be poorly fit

Table 2.2: Number of galaxies in each population which had walker positions discarded due to low probability in order to exclude those galaxies from the analysis which were poorly fit by this quenching model.

	Red Sequence	**Green Valley**	**Blue Cloud**
All walkers discarded	1420 (7.00%)	437 (2.41%)	3109 (5.37%)
More than half walker positions discarded	2010 (9.92%)	779 (4.30%)	6669 (11.52%)

by a quenching model (see Section **??**). This raises the issue of whether we exclude a significant fraction of our galaxy sample and whether those galaxies reside in a specific location of the colour-magnitude. The fraction of galaxies which had all or more than half of their walker positions discarded due to low probability are shown in Table 2. Using this constraint, 2.4%, 7.0% and 5.4% of green, red and blue galaxies respectively had *all* of their walker positions discarded.

This is not a significant fraction of either population, therefore this shows that the STARPY module is effective in fitting the majority of galaxies and that this method of discarding walker positions ensures that poorly fit galaxies are removed from the analysis of the results. Figure 2.4 shows that these galaxies with discarded walker positions are also scattered across the optical-NUV colour-colour diagram and therefore STARPY is also effective in fitting galaxies across this entire plane.

The Markov Chain positions are then binned and weighted by their corresponding logarithmic posterior probability $\log[P(\theta_k|d_k)]$, provided by the *emcee* package, to further emphasise the features and differences between each population in the visualisation. The GZ2 data also provides uniquely powerful continuous measurements of a galaxy's morphology, therefore we utilise the user vote fractions to obtain separate model parameter distributions for both smooth and disc galaxies. This is obtained by also weighting by the morphology vote fraction when the binned positions are summed. We stress that this portion of the methodology is a non-Bayesian visualisation of the combined individual galaxy results for each population.

For example, the galaxy shown in Figure 2 would contribute almost evenly to both the smooth and disc parameters due to the GZ2 vote fractions. Since galaxies with similar vote fractions contain both a bulge and disc component, this method is effective in incorporating intermediate galaxies which are thought to be crucial to the morphological changes between early- and late-type galaxies. It was the consideration of these intermediate galaxies which was excluded from the investigation by S14.

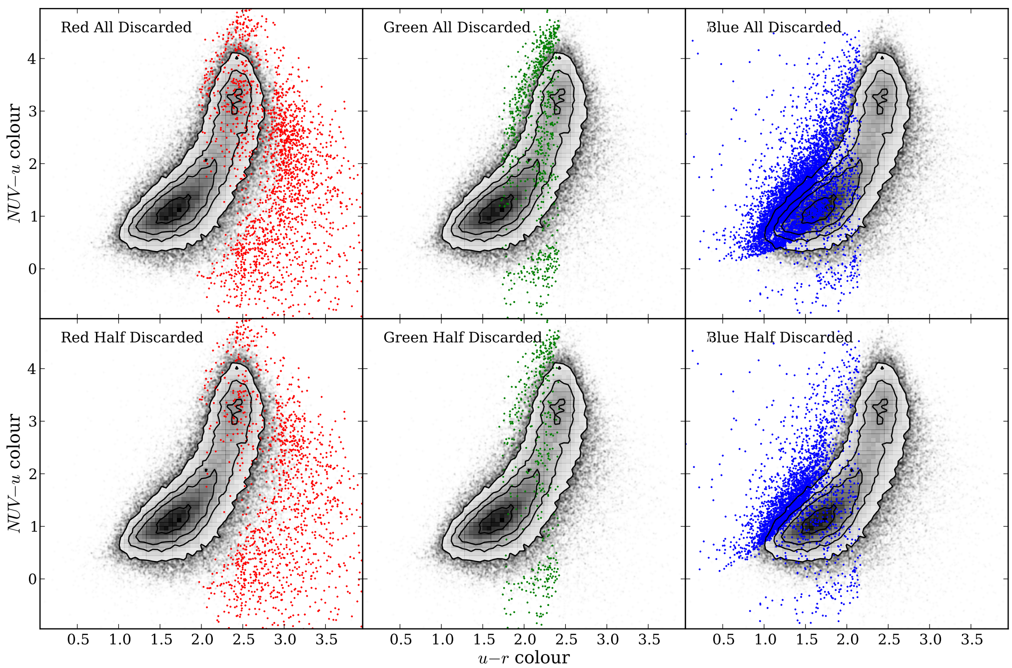

Figure 2.4: Contours show the full GZ2 subsample optical-NUV colour-colour diagram. The points show the positions of the galaxies which had all (top panels) or more than half (bottom panel) of their walker positions discarded due to their low probability for the red sequence (left), green valley (middle) and blue cloud (right).

Chapter 3

The morphological dependance of quenching

The work in the following chapter has been published in Smethurst et al. (2015).

Quenching is morphologically dependant.

Chapter 4

The Influence of AGN Feedback

The work in the following chapter has been published in Smethurst et al. (2016).

AGN can have a big impact on a galaxy.

4.0.1 Bulgeless galaxies hosting growing black holes

Chapter 5

The influence of the group environment

Mass quenching more important. Environment somewhat but not ram pressure stripping.

Chapter 6

Discussion

This is where I blow the lid of quenching. Bring it all together in a big happy family picture.

Chapter 7

Conlusions

Quenching is morphologically dependant.

AGN may be responsible for some of this quenching.

The environment plays less of a role than typical mass quenching.

Bibliography

Baldry I. K., Balogh M. L., Bower R. G., Glazebrook K., Nichol R. C., Bamford S. P., Budavari T., 2006, MNRAS, 373, 469

Bamford S. P. et al., 2009, MNRAS, 393, 1324

Brammer G. B. et al., 2009, ApJ, 706, L173

Croton D. J. et al., 2006, MNRAS, 365, 11

Darg D. W. et al., 2010, MNRAS, 401, 1043

Di Matteo T., Springel V., Hernquist L., 2005, Nature, 433, 604

Dressler A., 1980, ApJ, 236, 351

Goodman J., Weare J., 2010, CAMCS, 5, 65

Hickox R. C. et al., 2009, ApJ, 696, 891

Lintott C. et al., 2011, MNRAS, 410, 166

Lintott C. J. et al., 2009, MNRAS, 399, 129

Nandra K. et al., 2007, ApJ, 660, L11

Skibba R. A. et al., 2009, MNRAS, 399, 966

Smethurst R. J. et al., 2016, MNRAS

Smethurst R. J. et al., 2015, MNRAS, 450, 435

Willett K. W. et al., 2013, MNRAS, 435, 2835